Journal of Applied Electrochemistry **29**: 601–609, 1999.

Role of indium ions on the activation of aluminium

H. A. EL SHAYEB, F. M. ABD EL WAHAB and S. ZEIN EL ABEDIN
Electrochemistry and Corrosion Laboratory, National Research Centre, Dokki, Cairo, Egypt

Received 14 January 1998; accepted in revised form 10 September 1998

Key words: activation, aluminium, chloride, dissolution, impurities, indium, iron

Abstract

The effect of indium ions on the dissolution of aluminium in chloride solutions as well as the role of impurities normally present were investigated. Electrochemical techniques complemented by SEM and EDAX were utilized for two types of aluminium, Al_I(99.999%) and Al_{II}(99.61%). The activation process depends on the chloride ion concentration as well as the surface finish of the samples. Activation is attributed to deposition of In at the surface forming In–Al alloy which is responsible for Cl^- ion adsorption at high negative potentials (i.e., activation). Deactivation was exhibited in the case of Al_{II} due to the presence of Fe as an impurity. The effect of addition of Fe^{3+} alone, and together with In^{3+}, on the activation of Al_I in 0.6 M NaCl was also examined.

1. Introduction

Aluminium and aluminium alloys owe their corrosion resistance to complex oxide films formed irreversibly [1]. These films act as a barrier to the environment and retard corrosion even though the thermodynamic driving force towards metal dissolution still remains. Unalloyed aluminium, therefore, is electrochemically too passive for employment as an anode material in batteries or as a sacrificial anode in cathodic protection of steel in sea water.

Considerable effort has gone into the production of aluminium alloys which are electrochemically active. Elements such as indium [2–6], gallium [7, 8], zinc [4, 9] and tin [10–13] have been added as alloying elements for this purpose. Aluminium is also activated by In^{3+}, Ga^{3+} and Hg^{2+} ions in chloride solutions [14–19]. It seemed of interest to examine the effect of In^{3+} ions on the electrochemical behaviour of aluminium in chloride solutions using electrochemical and surface analytical techniques. Two types of aluminium were used; one Al_I 99.999% and the other Al_{II} 99.61% to demonstrate the role of minute impurities, for example, iron, on the activation process. The present study also aimed to add to the understanding of the mechanism of activation.

2. Experimental details

Measurements were made on ultrapure Al 99.999% (Al_I) and Al 99.61% (Al_{II}) containing 0.225% Fe, 0.109% Si and 0.013% Cu as impurities. The electrodes were abraded successively with metallographic emery paper of increasing fineness up to 800, then degreased with acetone and washed with running distilled water. The electrodes were cathodically polarized at −1900 mV vs SCE for 3 min in the electrolyte (0.6 M NaCl) before polarization and potentiostatic current–time measurements. The electrochemical cell was made of Pyrex glass fitted with a platinum auxiliary electrode separated from the electrolyte by a sintered glass diaphragm, and a saturated calomel reference electrode (SCE). All solutions were prepared from Analar grade reagents and distilled water.

Polarization measurements were made using a potentioscan (Wenking model POS 73). The electrode potential was changed in steps of 40 mV min^{-1} in the positive direction up to the breakdown potential. Potentiostatic current–time tests were carried out using a potentiostat–galvanostat (Amel model 2053) with an X–Y recorder (Kipp and Zonen). The treated electrodes were passivated in the electrolyte at −1050 mV in the case of Al_I and −950 mV in the case of Al_{II}, for 20 min. Appropriate amounts of dissolved $InCl_3$ or $FeCl_3$ salts were then added to the electrolyte maintaining the Cl^- ion concen-

tration constant. The solution was agitated slowly by a magnetic stirrer to mix the additives with the electrolyte. A scanning electron microscope (SEM: JSM T20, Joel Co. Ltd, Japan) and energy dispersive X-ray analyser (EDAX) were used to examine the electrode surface.

3. Results and discussion

The polarization behaviour of 99.999% Al(Al_I) and 99.61% Al(Al_{II}) in 0.6 M NaCl solution without and with different concentrations of In^{3+} were investigated; the results are shown in Figure 1. The polarization curve of pure aluminium (Al_I), Figure 1(a), is characterized by a flat passive region extending from −1600 to −780 mV, with a very low passive current density of 3 $\mu A\,cm^{-2}$ showing the passive behaviour of aluminium and revealing the stability of the oxide film [20] in this medium. The end of the passive region represents the breakdown potential, at which the onset of pitting takes place. The effect of impurities on the electrochemical behaviour of aluminium is clearly seen from the polarization curve of Al_{II} in 0.6 M NaCl, Figure 1(a), in which the cathodic arm of the curve moves to higher current densities and the corrosion potential takes a less negative value, −1280 mV, indicating the depolarization of cathodic reactions. The passive current density and the breakdown potential were observed at 115 $\mu A\,cm^{-2}$ and −680 mV, respectively.

The effect of adding increasing amounts of In^{3+} to 0.6 M NaCl on the polarization curves of Al_I and Al_{II} is displayed in Figure 1(b) and (c), respectively. The pitting potential of Al_I, Figure 1(b), moves to more negative values and, consequently, diminution of the passive region takes place with increasing concentration of In^{3+}. There is also a shift in E_{corr} to more positive values approaching the reversible potential for the In/In_2O_3 couple with increase in In^{3+} content. The reduction step observed on the cathodic branch of the polarization curves at higher concentrations of indium ions is due to the deposition of indium at the electrode surface in addition to the increased H^+ ion concentration according to the hydrolysis reaction:

$$In^{3+} + 3\,H_2O \rightleftharpoons In(OH)_3 + 3\,H^+ \qquad (1)$$

Almost similar results were obtained in the case of Al_{II} under the same conditions. There is a shift in the breakdown potential of Al_{II} towards the negative direction with increasing concentration of indium ions reaching values close to the corrosion potential at $C \geqslant 10^{-3}$ M In^{3+}, Figure 1(c).

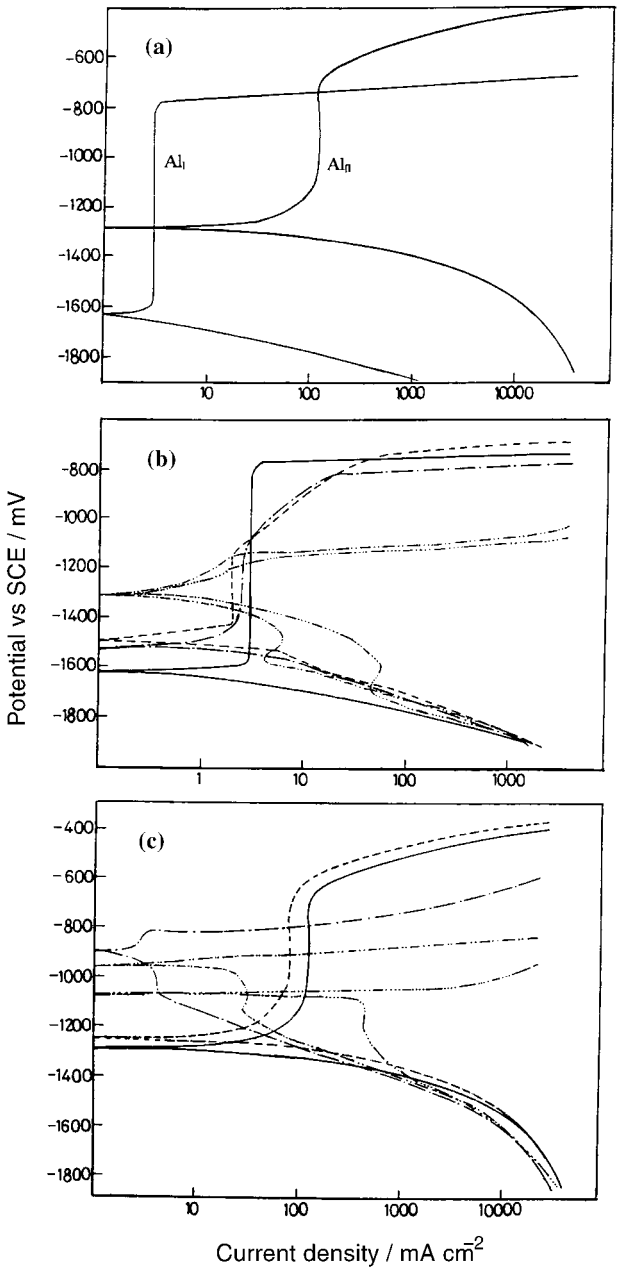

Fig. 1. (a) Polarization curves of Al_I and Al_{II} electrodes in 0.6 M NaCl. (b) Polarization curves of Al_I electrode in 0.6 M NaCl and different concentrations of In^{3+}. Curves (——) without In^{3+}, (- - - - -) 10^{-4} M In^{3+}, (— · —) 10^{-3} M In^{3+}, (—··—) 3×10^{-3} M In^{3+}, and (—·····—) 10^{-2} M In^{3+}. (c) Polarization curves of Al_{II} electrode in 0.6 M NaCl and different concentrations of In^{3+}. Curves (——) without In^{3+}, (- - - - -) 10^{-4} M In^{3+}, (— · —) 10^{-3} M In^{3+}, (—··—) 3×10^{-3} M In^{3+}, and (—·····—) 10^{-2} M In^{3+}.

The potentiostatic current–time measurements give additional valuable information about aluminium activation by indium salts. Figure 2 shows the current–time decay profiles of Al_I polarized at −1050 mV (which is in

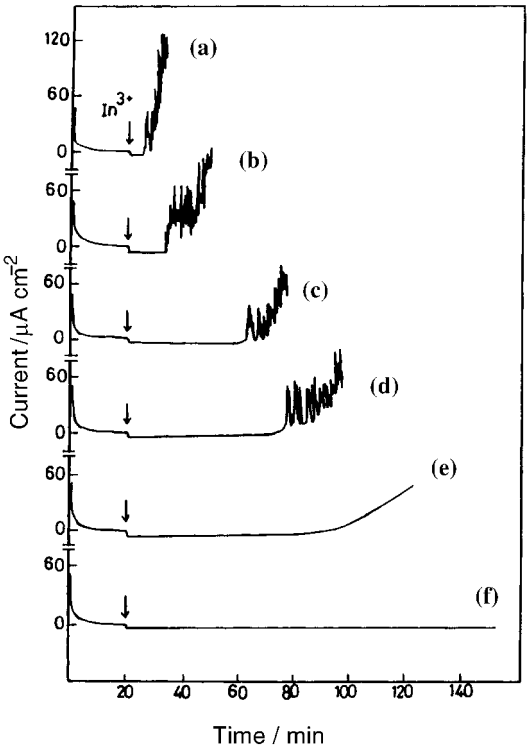

Fig. 2. Current–time curves for Al_I electrode passivated at -1050 mV in 0.6 M NaCl solution to which different concentrations of In^{3+} were added after 20 min: (a) 10^{-2}, (b) 7×10^{-3}, (c) 5×10^{-3}, (d) 2×10^{-3}, (e) 1×10^{-3} and (f) 1×10^{-4} M.

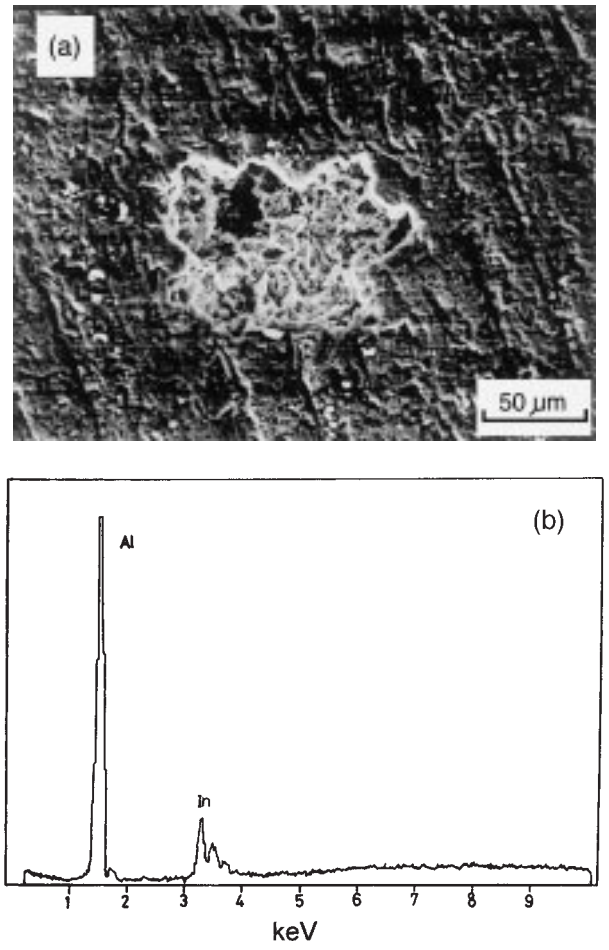

Fig. 3. (a) SEM micrograph of Al_I electrode obtained after potentiostatic polarization at -1050 mV in 0.6 M NaCl + 5×10^{-3} M In^{3+}. (b) EDAX analysis inside the pit shown in the micrograph.

the passive range) in 0.6 M NaCl solution to which a definite amount of In^{3+} was added after 20 min. A rapid decrease in the anodic current to zero was observed in the early moments of passivation. The current then becomes constant, indicating the formation of a passive film. The addition of In^{3+} ions causes no immediate effect and the current remains constant for a certain time corresponding to an induction period before activation. After the induction period the anodic current surges and suddenly increases, displaying fluctuations, indicating the start of passivity breakdown. As shown from the curves, at $C = 10^{-4}$ M In^{3+} no activation is observed while at $C \geqslant 10^{-3}$ M, the tendency to activation depends strongly on In^{3+} concentration and the induction period decreases with increase in In^{3+} concentration. Attack appears to be localized after passivity breakdown. This can be confirmed by SEM–EDAX examination of the electrode surface shown in Figure 3. The scanning electron micrograph, Figure 3(a), shows the surface morphology of the Al_I electrode after breakdown of passivity during potentiostatic conditions in 0.6 M NaCl solution containing 5×10^{-3} M In^{3+}. The surface exhibits crystallographic pitting attack with a high concentration of indium within the pits as detected by the corresponding EDAX analysis, Figure 3(b). Invariably, all the pits on the electrode surface were found to contain indium.

It seemed of interest to examine the effect of chloride ion concentration on the measured induction period for the activation of Al_I by addition of, for example, 5×10^{-3} M, In^{3+} during potentiostatic current–time measurements. It is clear that the increase in Cl^- ion concentration increases the extent of activation of Al_I indicating a synergistic effect between Cl^- and In^{3+} ions. The relation between the measured induction period and the Cl^- ion concentration is linear, Figure 4. The existence of a synergistic effect between indium and chloride ions has been observed previously [2, 21].

The extent of activation of Al_I under similar potentiostatic conditions was found to be affected by the surface finish of the samples. The relation between the measured induction period and the grade of metallo-

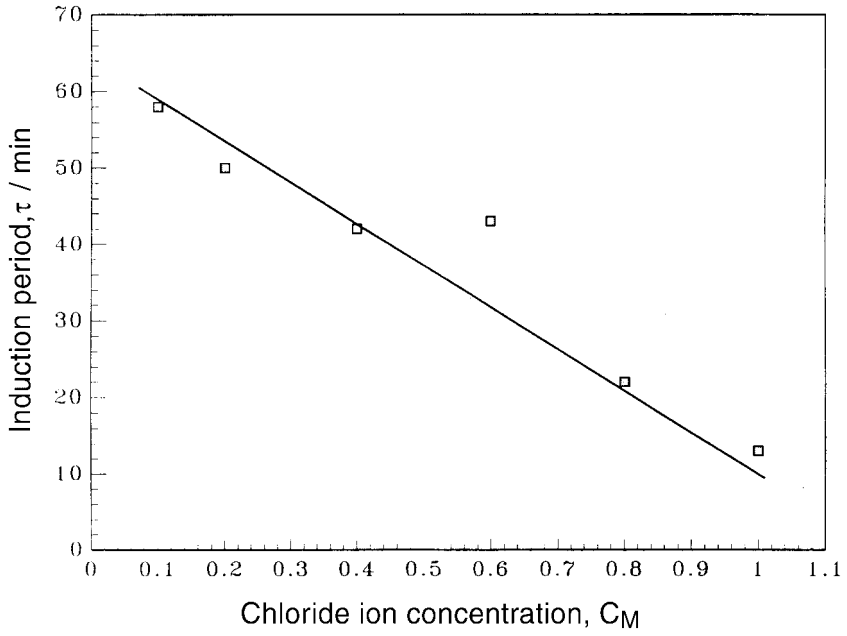

Fig. 4. Relation between chloride ion concentration and the induction period measured on activation of Al_I by 5×10^{-3} M In^{3+} at applied potential −1050 mV.

graphic silicon carbide papers used for polishing is shown in Figure 5 during the activation of Al_I by 5×10^{-3} M In^{3+} at −1050 mV in 0.6 M NaCl. It is clear that the induction period increases with decrease in surface roughness of the electrode. At high roughness the number of defect centres of the passive film increase. These centres act as active sites, where electrons are generated by aluminium oxidation; thus deposition of indium takes place at these sites resulting in high indium concentrations along the electrode surface which be-

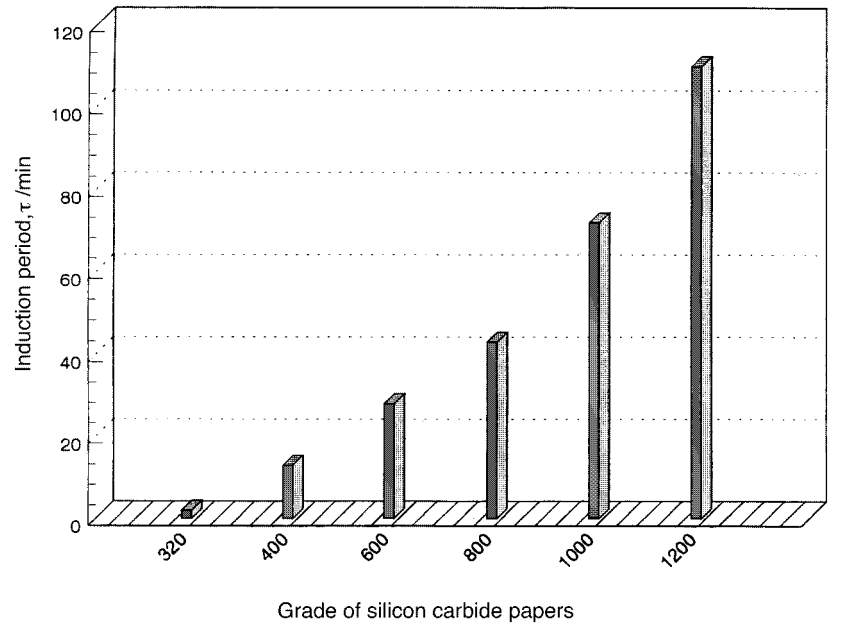

Fig. 5. Relation between the grade of silicon carbide papers and the induction period measured on activation of Al_I by 5×10^{-3} M In^{3+} in 0.6 M NaCl at applied potential −1050 mV.

come incorporated into the surface layers. Therefore, the activation process takes less time to occur. On the other hand, the quality of the passive film improves with use of fine silicon carbide paper; here the defect centres in the oxide film decrease in number and the activation process is delayed to larger times.

In the light of the above results it can be seen that there is an interrelationship between In^{3+} and Cl^- ions in the activation process, i.e., at constant Cl^- concentration the extent of activation increases with In^{3+} concentration and at constant In^{3+} concentration, activation increases with Cl^- content. Moreover, the activation process is strongly dependent on the surface finish of the samples.

The potentiostatic current-time measurements for Al_{II} (99.61% Al) in 0.6 M NaCl solution were also examined. The electrode was passivated at −950 mV (which is in the passive range) for 20 min, after which a definite amount of indium salt was added. The curves obtained, Figure 6, show different behaviour than that of Al_I. Before addition of In^{3+} the curves exhibit a rapid decrease in the anodic current with fluctuations having an amplitude of approximately 15 μA, indicating that the electrode is not completely passivated. This can be attributed to the impurities present in the aluminium (e.g., Fe, Si, Cu). On addition of indium salt to the solution, after 20 min, the cathodic current increases rapidly to an extent depending on In^{3+} concentration. At lower concentrations of In^{3+}, the cathodic current increases and remains constant for the duration of the experiment. At higher concentrations (10^{-2} M), a larger increase in cathodic current occurs characterized by a small maximum: the current then remains constant for about 20 min. Following this a further step is recorded at a more cathodic current of $-1150\ \mu A\ cm^{-2}$. This is due to deposition of indium at the electrode surface. The presence of impurities in the aluminium enhances the deposition of indium at the cathodic sites. Figure 7 shows the results of SEM–EDAX examination of the surface of an Al_{II} electrode passivated at −950 mV in 0.6 M NaCl solution and 5×10^{-3} M In^{3+}. The deposition of a large amount of indium at the surface is clearly seen, Figure 7(a), where the deposit is analysed as indium by the corresponding EDAX profile, Figure 7(b). It should be mentioned that irrespective of the deposition of indium, activation does not occur.

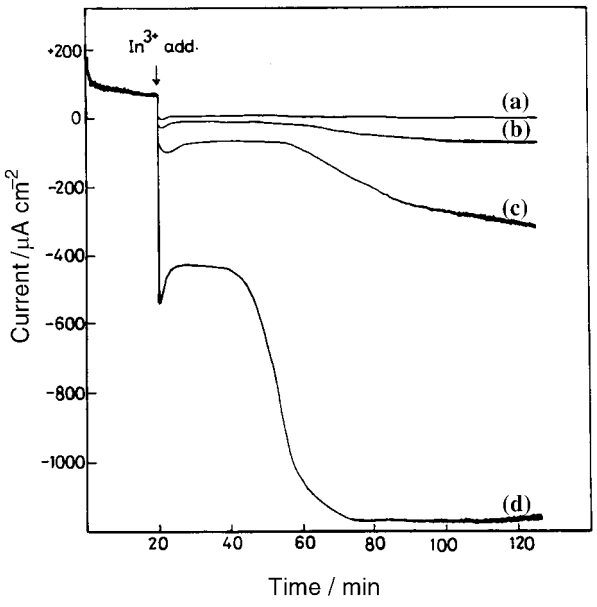

Fig. 6. Current–time curves for Al_{II} electrode passivated at −950 mV in 0.6 M NaCl solution to which different concentrations of In^{3+} were added after 20 min: (a) 1×10^{-4}, (b) 3×10^{-3}, (c) 5×10^{-3}, and (d) 1×10^{-2} M.

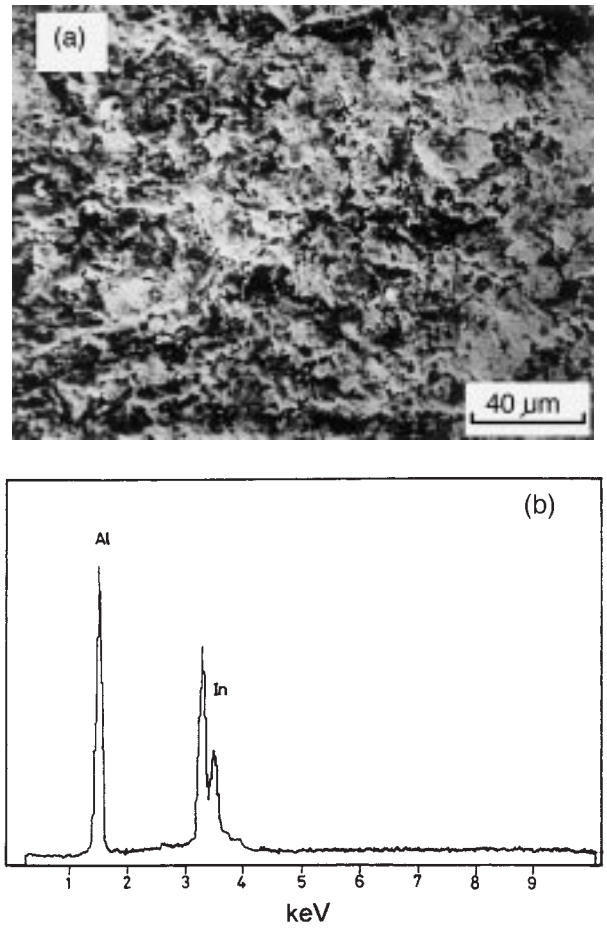

Fig. 7. (a) SEM micrograph of Al_{II} electrode obtained after potentiostatic polarization at −950 mV in 0.6 M NaCl + 5×10^{-3} M In^{3+}. (b) EDAX analysis of the area shown in the micrograph.

The deactivation observed on addition of indium ions to NaCl solutions in the case of Al_{II} can be attributed to the presence of impurities. By reference to the analysis of Al_{II}, it is clear that the major impurity is iron (0.225% Fe, 0.109% Si and 0.013 Cu). It is known [22–25] that the presence of iron in aluminium and aluminium alloys has detrimental effects on the performance of these alloys as sacrificial anodes in cathodic protection systems. This may be attributed to the blocking effect of Fe-precipitates on the diffusion of the activator alloying components [26]. Breslin et al. [27] suggested that the accelerated deposition of indium occurred on the surface of impure aluminium through the generation of indate solution formed due to the local high alkalinity of the solution adjacent to the Fe-precipitate regions. This deposited indium was rendered inactive due to the blocking effects exerted by Fe on the diffusion of indium into the aluminium matrix.

Based on the above discussion it appears that the activation of Al by indium is dependent on the impurities present. It is known that the amount, as well as the types, of impurities is a factor. Iron, for instance, hinders the diffusion of In into the surface layers of the electrode, preventing the true In/Al contact and hence masking the activation process. That no activation takes place is explained on the basis that the activation process of Al is accomplished only if the additives are incorporated in the outermost surface layer of aluminium [2, 15, 17, 27]. Therefore, it seemed of interest to examine the effect of different concentrations of Fe^{3+} in 0.6 M NaCl solution on the behaviour of ultrapure Al under potentiostatic conditions.

The curves of Figure 8 show the effect of different concentrations of Fe^{3+} ion on the behaviour of the Al_I electrode passivated at -1050 mV in 0.6 M NaCl solution and to which different concentrations of Fe^{3+} were added after 20 min. Addition of lower concentrations of Fe^{3+} ($10^{-3} \geqslant C > 10^{-5}$) causes a rapid increase in cathodic current and, after a definite time (induction period τ), the current increases in the anodic direction, with fluctuations, to attain an approximately constant value with frequency varying with Fe^{3+} ion concentration. The induction period increases with increasing Fe^{3+} ion concentration, showing an increase in the amount of deposited iron on the electrode surface. This process leads to a decrease in attack of the electrode due to its contamination with the deposited iron.

The scanning electron micrograph in Figure 9, shows the attacked area of the Al_I electrode by 10^{-4} M Fe^{3+} indicating localized attack with deep and heterogeneous heart-shaped pits. It has been reported that Fe^{3+} ions accelerate the corrosion of Al in solutions containing Cl^- by varying rates depending on the concentration of

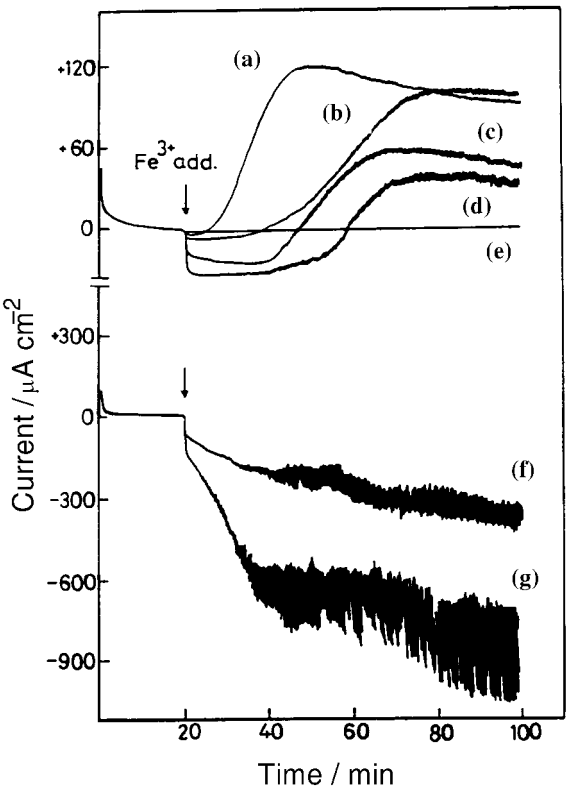

Fig. 8. Current–time curves for Al_I electrode passivated at -1050 mV in a 0.6 M NaCl solution to which different concentrations of Fe^{3+} ions were added after 20 min: (a) 5×10^{-5}, (b) 1×10^{-4}, (c) 5×10^{-4}, (d) 1×10^{-3} and (e) 1×10^{-5}, (f) 5×10^{-3} and (g) 1×10^{-2} M Fe^{3+}.

Fe^{3+} [28–30]. The activation observed at lower concentrations of Fe^{3+} may be due to deposition of a very low amount of Fe on the electrode surface, which cannot be detected by EDAX analysis, but was able to change the

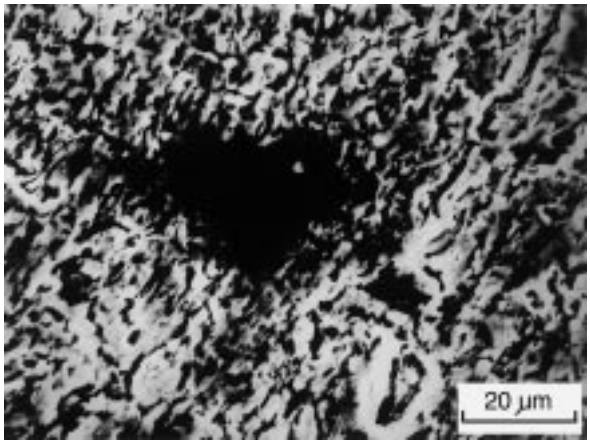

Fig. 9. SEM micrograph of Al_I electrode obtained after potentiostatic polarization at -1050 mV in 0.6 M NaCl + 10^{-4} M Fe^{3+}.

nature of the oxide film. At higher concentrations of Fe^{3+} ($C \geqslant 5 \times 10^{-3}$ M), on the other hand, the cathodic current increases rapidly towards negative values and becomes fluctuating with increase in magnitude and frequency with increase in Fe^{3+} concentration. This behaviour is due to deposition of iron on the electrode surface, as shown by EDAX analysis and the SEM micrograph, Figure 10. The deposited layer causes passivation of the electrode, leading to reduced activation by indium. Therefore, the electrode, after deposition of Fe, was subjected to the same experimental conditions as those imposed on Al_I, that is, passivated at -1050 mV in 0.6 M NaCl and to which 5×10^{-3} M In^{3+} was added after 20 min.

As indicated in Figure 11, there is a rapid increase in the cathodic current due to deposition of indium at the electrode surface. However, the current is characterized by a comparatively long induction period of 135 min., followed by an increase in anodic current with fluctuations indicating passivity breakdown. The value of anodic current after passivity breakdown is low in both frequency and magnitude compared to that obtained for the untreated electrode under the same conditions. Consequently, the presence of an Fe-deposited layer on the electrode surface delays the activation process, but does not prevent it completely, for the deposited iron does not diffuse into the aluminium matrix to act as an impurity in the aluminium.

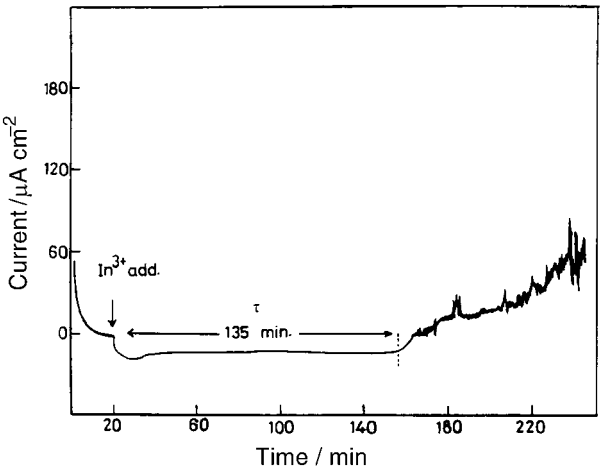

Fig. 11. Current–time curve for Al_I electrode (used after passivation at -1050 mV in 0.6 M NaCl and 10^{-2} M Fe^{3+} for 120 min) passivated at -1050 mV in 0.6 M NaCl and to which 5×10^{-3} M In^{3+} was added after 20 min.

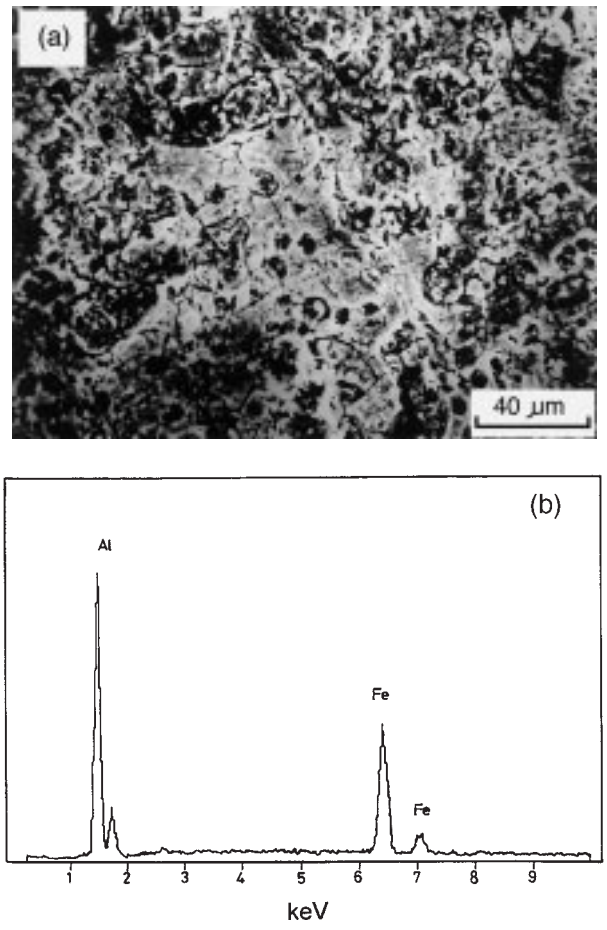

Fig. 10. (a) SEM micrograph of Al_I electrode obtained after potentiostatic polarization at -1050 mV in 0.6 M NaCl + 10^{-2} M Fe^{3+}. (b) EDAX analysis of the area shown in the micrograph.

The effect of addition of Fe^{3+} and In^{3+} ions at the same time was studied. On the one hand, it is clear from the potentiostatic I/t curves, Figure 12, that increasing the amount of Fe^{3+} ion at constant In^{3+} ion concentration (5×10^{-3} M In^{3+}) leads to a diminution of the induction period and hence accelerates the electrode activation. On the other hand, increasing the In^{3+} ion concentration at constant Fe^{3+} ion concentration (10^{-2} M) causes a shift of the cathodic current towards less negative values, Figure 13. At higher In^{3+} concentrations, $C \geqslant 3 \times 10^{-3}$ M, activation of the electrode takes place depending on the indium ion content in the solution.

The outcome of the above experiments shows that addition of Fe^{3+} ion alone (10^{-2} M) causes passivation and after addition of In^{3+}, activation then takes place. This may be attributed to exchange reactions between aluminium and the added ions as follows:

$$Al + In^{3+} \rightleftharpoons Al^{3+} + In \quad (2)$$

$$Al + Fe^{3+} \rightleftharpoons Al^{3+} + Fe \quad (3)$$

Thermodynamically, indium is expected to be deposited preferentially. However, at low In^{3+} concentrations there will be some bare areas on the electrode permitting

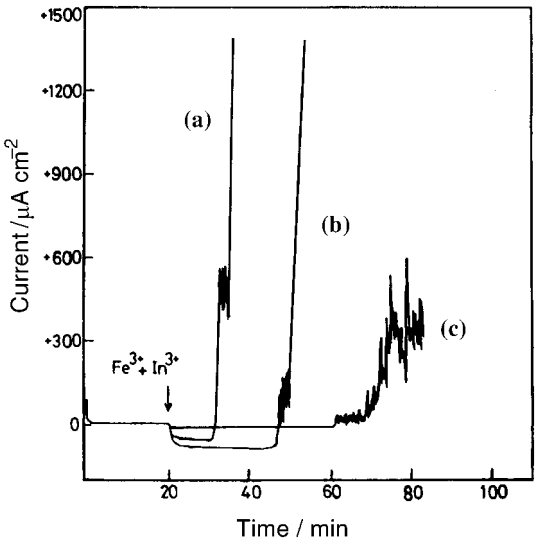

Fig. 12. Effect of Fe^{3+} ion concentration on the activation of Al_I in presence of 5×10^{-3} M In^{3+} during potentiostatic polarization at -1050 mV in 0.6 M NaCl: (a) 1×10^{-2}, (b) 5×10^{-3} and (c) 0.0 M Fe^{3+}.

Fe^{3+} to react and Fe to be also deposited. Thus, at higher content of In^{3+}, its role is predominantly activation while, in contrast, at higher Fe^{3+} content passivation occurs.

4. Activation mechanism

The activation mechanism is complex. Deposition of indium on the electrode surface is the initial stage, as shown from the micrograph of Figure 14 taken during the induction period prior to activation. The deposition occurs at defect centres or flaws in the aluminium oxide film. Richardson and Wood [31] reported that all oxide films on aluminium contain flaws. During the passivation of the aluminium electrode in 0.6 M NaCl at -1050 mV, species such as $Al(OH)Cl^{+}$ and $AlCl^{++}$ may exist, giving rise to the relatively stable $Al(OH)_2Cl$ complex, reported in pit initiation studies [32, 33]. The incorporation of these complexes into the developing film may result in the generation of flaws at which deposition of indium occurs. Aluminium activation is attained only when indium deposition process takes place within an active pit, producing a true In/Al metallic contact and formation of In–Al alloy at the surface [2, 17]. Nevertheless, if deposition occurs on the oxide, no activation is observed. In the case of Al_I the deposition of In occurs at flaws which act as active sites on the oxide film enabling a true In/Al contact with local formation of In–Al alloy at the surface, so that activation occurs. In the case of Al_{II}, indium deposited at cathodic sites which mainly arise from cathodic impurities normally present in the aluminium matrix, and true In/Al metallic contact does not occur, hence preventing activation.

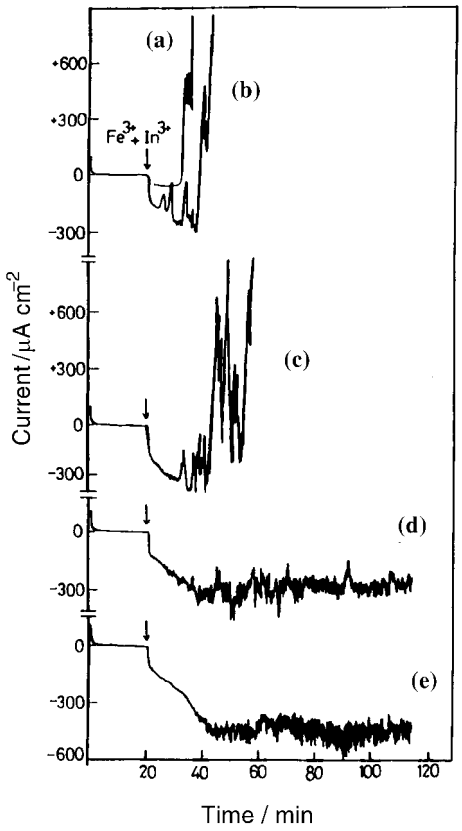

Fig. 13. Current–time curves of Al_I electrode passivated at -1050 mV in 0.6 M NaCl to which 10^{-2} M Fe^{3+} + different concentrations of In^{3+} were added after 20 min: (a) 5×10^{-3}, (b) 4×10^{-3}, (c) 3×10^{-3}, (d) 2×10^{-3} and (e) 1×10^{-3}, M In^{3+}.

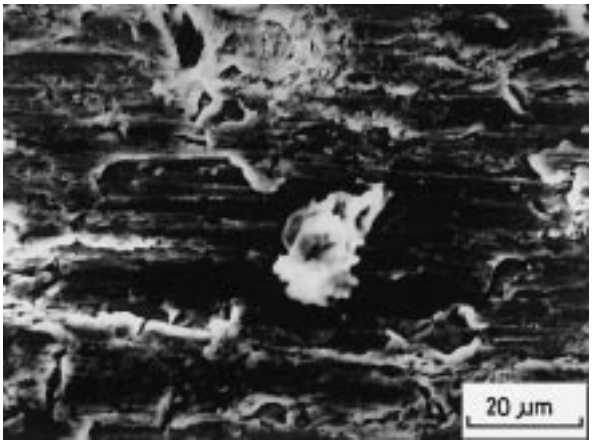

Fig. 14. SEM micrograph of Al_I electrode passivated at -1050 mV in 0.6 M NaCl + 3×10^{-3} M In^{3+} before activation.

It has been stated [34] that the potential of zero charge, E_{PZC}, for indium metal in 10^{-2} M KCl containing 10^{-3} M HCl is -0.9 V and combining this with the greater affinity of In for Cl^- [35], gives rise to a high surface concentration of Cl^-. Moreover, there is excess of Cl^- inside a pit. Thus, once a sufficient amount of indium metal has been deposited on the defect centres of the oxide film and an In/Al surface is formed, the surface Cl^- ion concentration increases and approaches that observed at the pitting potential. It is known that the surface concentration of Cl^- increases from 3% at the open circuit potential to 12–13% at the critical pitting potential [36]. Accordingly, and consistent with our results, it is clear that Cl^- ion adsorption takes place at a more electronegative potential in the presence of In^{3+}.

5. Conclusions

The outcome of the present investigation can be summarized as follows:

(i) Activation of Al_I (99.999%) in chloride solution by indium is strongly dependent on the chloride ion concentration, as well as the surface finish of the samples.

(ii) In the case of Al_{II} (99.61%), deactivation observed on addition of In^{3+} ions is due to the presence of the minor impurities, especially iron, which hinders the diffusion of indium into the surface layers of the electrode.

(iii) The addition of Fe^{3+} ion to the electrolyte accelerates the dissolution of Al_I by varying amounts, depending on the concentration of Fe^{3+}. At constant In^{3+} concentration, the degree of activation of Al_I increases with increase in Fe^{3+} concentration.

(iv) The activation process occurs due to deposition of In at oxide flaws enabling a true In/Al contact to be generated due to formation of an In–Al alloy at the surface which leads to Cl^- ion adsorption at potentials more electronegative than at aluminium. However, in the case of deactivation, the deposition of In takes place on the oxide layer and/or at the impurities themselves, thus preventing direct contact of In with the electrode.

References

1. P.A. Malachesky, *in* 'Encyclopedia of Electrochemistry of the Elements' Vol. 6, Edited by A.J. Bard (Marcel Dekker, NewYork, 1976), p. 63.
2. S.B. Saidman, S.G. Garcia and J.B. Bessene, *J. Appl. Electrochem.* **25** (1995) 252.
3. C.B. Breslin and W.M. Carroll, *Corros. Sci.* **34** (1993) 1099.
4. C.B. Breslin and W.M. Carroll, *Corros. Sci.* **36** (1994) 85.
5. L. Bai and B.E. Conway, *J. Appl. Electrochem.* **22** (1992) 131.
6. A. Venugopal and V.S. Raja, *Br. Corros. J.* **31** (1996) 318.
7. C.B. Breslin and W.M. Carroll, *Corros. Sci.* **33** (1992) 1735.
8. C.D.S. Tuck, J.A. Hunter and G.M. Scamans, *J. Electrochem. Soc.* **134** (1987) 2070.
9. M.C. Reboul, PH. Gimenez and J.J. Rameau, *Corrosion* **40** (1984) 366.
10. M. Kliškić, J. Radošević and LJ.Aljinović, *J. Appl. Electrochem.* **24** (1994) 814.
11. A. Venugopal, P. Veluchamy, P. Selvam, H.Minoura and V.S. Raja, *Corrosion*, **53** (1997) 808.
12. T. Valand and G. Nilsson, *Corros. Sci.* **17** (1977) 931.
13. D.R. Salinas and J.B. Bessone, *Corrosion,* **47** (1991) 665.
14. S.B. Saidman and J.B. Bessone, *J. Appl. Electrochem.* **27** (1997) 731.
15. *Idem*, *Electrochim. Acta* **42** (1997) 413.
16. F. Holzer, S. Müller, J. Desilvestro and O. Haas, *J. Appl. Electrochem.* **23** (1993) 125.
17. G. Burri, W. Luedi and O. Haas, *J. Electrochem. Soc.* **136** (1989) 2167.
18. J.U. Chavarin, *Corrosion*, **47** (1991) 472.
19. W.M. Carroll and C.B. Breslin, *Br. Corros. J.* **26** (1991) 255.
20. P. Li. Cabot, J.A. Garrido, E. Perez and J. Vingili, *Corros. Sci.* **26** (1986) 5.
21. W.M. Carroll and C.B. Breslin, *Corros. Sci.* **33** (1992) 1161.
22. B.M. Ponchel and R.L. Horst, *Mater. Protect.* **7** (1968) 38.
23. T. Sakano, K. Toda and M. Hamado, *Mater. Protect.* **5** (1966) 45.
24. A. Michajlovic, A. Mance and O. Nesic, *J. Serb. Chem. Soc.* **52** (1987) 663.
25. P.J. Knuckey and B.S. Smith, 'Interinsic Factors Affecting Aluminium Alloy Anode Performance', paper 2 *in* Proceedings of the 5th International Wave Corrosion Conference (1976) 26/1–26/13.
26. A.R. Despić, R.M. Stevanović and A.M. Vorkapić, 'A New Method of Obtaining Electrochemically Active Aluminium', paper A2-19, Extended Abstracts, 35th ISE Meeting, Berkeley, CA, Aug. (1984).
27. C.B. Breslin, L.P. Friery and W.M. Carroll, *Corrosion* **49** (1993) 895.
28. M.G.A. Khedr and A.M.S. Lashien, *Corros. Sci.* **33** (1992) 137.
29. M.M. Badran and E.A. Abd El-Meguid, *Egypt. J. Chem.* **35** (1992) 625.
30. D. Wong, L. Swette and F.H. Cocks, *J. Electrochem. Soc.* **126** (1979) 11.
31. J.A. Richardson and G.C. Wood, *Corros. Sci.* **10** (1970) 313.
32. T.H. Nguyen and R.T. Foley, *J.Electrochem. Soc.* **26** (1979) 1855.
33. L. Tomcsanyi, K. Varga, I. Bartik, G. Haronyi and E. Maleczki, *Electrochim. Acta* **34** (1989) 855.
34. Z.A. Rotenberg and Yu. V. Pleskov, *Electrochimiya* **9** (1973) 1419.
35. F.A. Cotton and G. Wilkinson, 'Advanced Inorganic Chemistry', 4th edn (J. Wiley and Sons, New York, 1980), p. 334.
36. J. Augustynski, *in* 'Passivity of Metals', edited by R.P. Frankenthal and J. Kruger, Electrochemical Society, Pennington, NJ 1987, p. 989.